Iranian Journal of Basic Medical Sciences
ijbms.mums.ac.ir

Combining sorafenib and *Lactobacillus rhamnosus* GG reduces liver fibrosis and hepatic encephalopathy following bile duct ligation in rats

Tina Rahjoo [1, 2], Ghorbangol Ashabi [2], Soheila Adeli [1], Shahnaz Halimi [3], Mahshid Panahi [4], Omid Reza Tamtaji [2], Reihaneh Ghasemi-tarie [2], Fatemeh Nabavizadeh [1, 2*]

[1] Electrophysiology Research Center, Neuroscience Institute, Tehran University of Medical Sciences, Tehran, Iran
[2] Department of Physiology, School of Medicine, Tehran University of Medical Sciences, Tehran, Iran
[3] Department of Microbiology, School of Medicine, Tehran University of Medical Sciences, Tehran, Iran
[4] Department of Pathology, Firoozgar Hospital, Iran University of Medical Sciences, Tehran, Iran

ARTICLE INFO

Article type:
Original

Article history:
Received: Sep 27, 2025
Accepted: Mar 3, 2026

Keywords:
Hepatic encephalopathies
Lactobacillus rhamnosus
Liver fibrosis
Probiotic
Sorafenib

ABSTRACT

Objective(s): Liver fibrosis can progress to hepatic encephalopathy (HE). While sorafenib is a drug employed to treat liver fibrosis, its use is linked to drug resistance and adverse effects. We examined the potential benefits of combining sorafenib with the probiotic *Lactobacillus rhamnosus* GG (LGG) on liver fibrosis and HE in bile duct ligated (BDL) rats.

Materials and Methods: Forty male rats were randomly assigned to five groups of eight rats each, including sham, BDL, BDL+probiotic (LGG, 1×10^9 CFU/ml/day), BDL+sorafenib (20 mg/kg), and BDL+probiotic+sorafenib. First, rats received probiotic LGG or solvent for 2 weeks. Following a one-week post-BDL recovery period, the animals received sorafenib and probiotic LGG for three consecutive weeks. Next, various parameters were appraised.

Results: The combination of sorafenib with LGG led to less liver fibrosis when compared with sorafenib alone. This combination therapy also alleviated inflammation and oxidative species present in the liver and frontal cortex. Further, this combination diminished hepatic Toll-like receptor 4/ Nuclear factor kappa-β expression. Finally, it led to improved cognitive function in behavioral assessments compared to using sorafenib alone.

Conclusion: Overall, combining a low dose of sorafenib with probiotic LGG may offer significant benefits for treating liver fibrosis and HE.

▶Please cite this article as:
Rahjoo T, Ashabi Gh, Adeli S, Halimi Sh, Panahi M, Tamtaji OR, Ghasemi-tarie R, Nabavizadeh F. Combining sorafenib and *Lactobacillus rhamnosus* GG reduces liver fibrosis and hepatic encephalopathy following bile duct Ligation in rats. Iran J Basic Med Sci 2026; 29:

Introduction

Chronic liver diseases represent a significant health challenge worldwide, contributing to around 2 million deaths annually (1). Liver damage results in the development of liver fibrosis, defined by an excess accumulation of collagen in the matrix outside the cells. This progressive damage can induce cirrhosis and hepatic cancer through a three-stage process of inflammation-fibrosis-carcinoma (2). The progression of liver fibrosis is influenced by several factors, such as the production of inflammatory signaling molecules, including Toll-like receptors (TLRs), interleukin-6 (IL-6), and tumor necrosis factor-alpha (TNF-α) (3). In those with liver fibrosis, the liver's diminished capacity to eliminate toxins, such as ammonia, leads to their accumulation in the brain. This ultimately causes brain dysfunction, known as hepatic encephalopathy (HE), which encompasses a wide range of central nervous system disorders. Symptoms can vary and may include confusion, altered consciousness, memory issues, and even coma. Although ammonia is regarded as a major factor in the pathophysiology of HE, several mechanisms also contribute to the condition including systemic inflammation and gut-brain axis disruption (4). Bile duct ligation (BDL) is an effective model for inspecting the progression of liver fibrosis and HE (5). In the BDL-induced HE model, cognitive deficits arise from impaired expression of brain-derived neurotrophic factor (BDNF), which is considered essential for cognitive functions, and is located in the frontal cortex, cerebral cortex, and hippocampus (6). Even though medications are recommended for managing liver fibrosis and HE, their side effects can make them intolerable for some patients, thus entailing novel therapeutic strategies.

Sorafenib has proved to suppress hepatic stellate cell proliferation by over 75% and down-regulate key fibrogenic genes such as TGFβ1, TIMP-1, and collagen I, leading to a significant decline in fibrosis in animal models (7).

***Corresponding author:** Fatemeh Nabavizadeh. Electrophysiology Research Center, Neuroscience Institute, Tehran University of Medical Sciences, Tehran, Iran. Tel: +98-21-66419484, Fax: +98-21-66419484, Email: nabavizadeh@tums.ac.ir

Sorafenib is approved for treating advanced hepatocellular carcinoma and other cancers; also, functioning as a multi-receptor tyrosine kinase inhibitor compound, it prevents tumor cell growth by affecting vascular endothelial growth factor (VEGF) (8). It also lowers collagen production and promotes collagen breakdown in hepatic stellate cells, significantly diminishing portal hypertension and new blood vessel formation in mice with liver fibrosis (9). Nevertheless, the use of sorafenib is linked to numerous side effects, including skin reactions on the hands and feet, weight loss, diarrhea, alopecia, anorexia, voice changes, and, in serious cases, high blood pressure, abdominal pain, neutropenia, thrombocytopenia, and lymphopenia. These side effects can result in discontinuation of the medication (10). Thus, there is a clear need to develop novel treatment approaches. Current research is actively exploring the combination of sorafenib with other drugs to lower its initial dosage.

Considering the crucial function of gut microbiota in the etiology of HE, it is critical to examine bacterial interventions that could potentially confer a protective effect against HE. Probiotics, defined as live bacteria, can be employed to address issues linked to the gut-liver interaction. Over the past decade, substantial advancements have been made in research on probiotic medications for addressing various liver disorders, demonstrating their benefits for liver fibrosis and HE (11). Probiotic supplementation, particularly with Bifidobacterium and Lactobacillus strains, enhances intestinal barrier function through up-regulating tight junction proteins such as occludin, which lowers intestinal permeability and limits lipopolysaccharide (LPS) translocation (12). This plays a key role in liver fibrosis, whereby gut barrier dysfunction allows LPS to move into the liver through the portal vein, activating the TLR4 pathway and driving fibrotic processes (13). Among probiotics, we specifically chose to focus on *Lactobacillus rhamnosus* GG (LGG). It is a highly studied probiotic strain with well-documented beneficial effects on gut-liver axis modulation, plus anti-inflammatory characteristics, both being highly relevant to liver fibrosis progression. LGG has been effective on boosting liver health and mitigating fibrosis-related inflammation in preclinical studies, making it a suitable candidate for combination with sorafenib in our investigation (14). For example, one study noted that LGG strengthened the intestinal barrier, resulting in diminished levels of alanine aminotransferase (ALT) associated with alcohol consumption (15). In a separate study, LGG intake lowered pro-inflammatory cytokines such as TNF-α and IL-6 in a BDL model. Research has also indicated that LGG inactivates the TLR4/NF-κB signaling cascades, which trigger generation of inflammatory mediators (16). Interestingly, probiotics linked to inflammation may alleviate abnormal behaviors, such as social withdrawal and immobility, in animals (17).

To date, there is no direct evidence that sorafenib and probiotics interact to modulate brain function via the gut–brain axis or that their combination has defined neuropharmacological effects. Given the significant advancements in probiotic research for various illnesses, including liver diseases, as well as their proven effectiveness in managing HE, the present study aims to determine whether combining sorafenib with the probiotic LGG offers protective effects against liver fibrosis, HE, and cognitive disorders in a BDL model in rats.

Materials and Methods

A total of 40 male Wistar rats (Pasteur Institute, Iran), weighing between 185 and 215 grams, were placed in a controlled environment with a temperature of 25±2 °C, regulated humidity, and a 12-hour light/dark cycle. The study protocol received approval from the local ethics committee at Tehran University of Medical Sciences (IR.TUMS.AEC.1402.011).

Induction of HE by BDL

Liver fibrosis was induced by BDL, representing HE caused by chronic liver disease. Following anesthetization by ketamine (90 mg/kgBW, intraperitoneally (IP)) and xylazine (9 mg/kgBW, IP), a vertical incision was made to locate and doubly ligate the common bile duct before cutting it. Within the sham group, the main bile duct was identified and exposed without being tied off. Rats were housed for four weeks post BDL surgery (5).

Experimental groups

In our study, 40 rats were separated into 5 groups (n = 8) to induce the chronic HE model. In the sham group, the animals were subjected to a surgical intervention akin to BDL surgery, except that the common bile duct was left intact and not ligated. In the BDL group, the rats were induced by BDL. In the probiotic LGG (PRO) group, the rats received probiotic LGG (1×109 CFU/ml/day) two weeks before BDL surgery. Following the recovery period (1 week), they received probiotic LGG with the same dose for three consecutive weeks. In the sorafenib (SOR) group, the rats were induced by BDL, and one week after surgery, they received sorafenib (20 mg/kg) for three consecutive weeks. In the probiotic LGG + sorafenib (PRO+SOR) group, the rats received probiotic LGG (1×109 CFU/ml/day) two weeks before BDL surgery. Following the recovery period (1 week), they received probiotic LGG (1×109 CFU/ml/day) and sorafenib (20 mg/kg) for three consecutive weeks.

Sorafenib treatment

Sorafenib tablets (Sevara ® 200 mg) were procured from Nanoalvand (Nanoalvand, Iran). After removing the outer coating, the tablet was ground and dissolved completely in tap water (18). Sorafenib (20 mg/kg) was administered through oral gavage once a day for three weeks after one week post-BDL (19).

Primary culture of bacteria

The Man–Rogosa–Sharpe (MRS) agar medium was employed to culture bacteria (Sigma Aldrich, USA). Given its acidic pH, MRS medium would present a selective feature for the growth of Lactobacillus. Initially, the bacteria storage vial was removed from the -70 °C freezer. About 10 microliters of bacterial suspension were inoculated on the MRS medium. The bacterial plate was placed inside an anaerobic jar, and an anoxomat device was then utilized to create and maintain conditions within the jar. After a 48-hour incubation period at a temperature of 37 °C, the bacterial culture plate was removed from the incubation jar.

Preparing the target concentration of bacteria

In order to create a suspension with a concentration of 109 CFU/ml, which is equivalent to half a McFarlane, a pure colony was removed from the second plate and inoculated into a sterile physiological saline solution. After

vortexing, the suspension's optical density was recorded at a wavelength of 620 nanometers, where the value should be equal to 0.1 (20).

Open field test

On day 27 post-surgery, the rats were placed in the dedicated behavioral testing room during the habituation phase to acclimate them to the experimental environment. The open field test was applied for evaluating overall levels of locomotor activity, anxiety, and exploratory behavior in animals such as rats. On day 28 post-surgery, an open field test was performed; the rats were located within a spacious square enclosure constructed from Plexiglas, measuring 80×80×50 cm. The test involved gradually positioning each animal in the arena's center, allowing them to roam freely for 5 min. The parameters ascertained included the entire distance moved (distance measured in centimeters), the frequency of times the animal ventured to the center zone, as well as the number of rearing (21).

Y-maze test

The Y-maze test is employed for appraising short-term memory performance. On day 28 post-surgery, a Y-maze test was performed. Specifically, the maze consisted of three arms, each measuring 40 cm in length, a height of 13 cm, and a bottom width of 3 cm, gradually widened to 10 cm at the top. The rats were strategically placed at the terminus of one arm and given the liberty to navigate through the maze for 10 min. The order in which the arms were introduced was documented, which may have involved revisiting the same arm multiple times. Alternation was described as entering all three study arms consecutively on each occasion. The maximum alternation count was obtained through subtracting two from the total number of arm entries. The actual number of alternations was divided by the maximum number of alternations minus 2. The outcome was multiplied by 100 to obtain the percentage of alternations using the formula: (actual alternations / (maximum alternations - 2)) × 100 (22).

Novel object recognition test (NORT)

On day 28 post-surgery, the NORT test was undertaken as follows: In a spacious square enclosure constructed from Plexiglas, measuring 80×80×50 cm, two similar objects were positioned at two edges, each 6 cm away from the border. In the initial phase, the rat engaged in unrestricted exploration for 5 min. Along the investigation, the time spent on each object was documented. Following a ten-minute interval, the rats were relocated to their cages. Next, in the second phase, a comparable trial was performed with a modification: one item was substituted with a new item that matched the original in size but differed in appearance. The time of exploration around the new object (NT) and familiar object (FT) was observed, with a recognition index (RI) also obtained through the formula [RI = (NT−FT)/ (NT+FT)]. Post every session, the equipment was thoroughly sterilized with a 75% ethanol solution to eliminate any lingering odors (23).

Passive avoidance test

On days 27–29 following the surgery, a passive avoidance test was conducted to ascertain the subject's memory following a fear response. On day 28, after completing the open field, Y-maze, and novel object recognition tests, the first step of this test was carried out. On day 29, the second stage was conducted. The test took place in a plastic chamber measuring 41×21×30 cm, featuring two sections- one light and one dark, split by a door. This test was performed following the established protocol. The duration taken for the rat to move from the light compartment into the dark compartment (known as the transfer latency) was noted. If the rat remained in the light compartment for the entire 10-minute test period, the recorded latency for the transfer was noted as 10 min (24).

PET and SPECT imaging

The small-animal positron emission tomography (PET) scans were conducted using a micro-PET scanner (Xtrim PET, IRAN) at the Preclinical Core Facility located at Tehran University of Medical Sciences. On day 29 post-surgery, following anesthesia, approximately 0.3 millicuries (mCi) of the radioactive tracer 18FDG (fluorodeoxyglucose labeled with fluorine-18) was administered to each rat through injection into the tail vein (25). Along each small animal PET scan, three-dimensional regions of interest (ROIs) surrounding the brain were manually defined. After background correction, the brain to background uptake ratio (BBR) was computed by the formula: (brain counts per voxel) / (background ROI counts per voxel) (26). Next, the single photon emission computed tomography (SPECT) radionuclide imaging was performed using a dual-headed small animal SPECT scanner (HiReSPECT, IRAN). The rats were administered approximately 2 mCi of the radioactive compound 99m Tc-phytate through an injection into their tail vein while being under general anesthesia. The region of interest (ROI) included the entire liver and the surrounding background, and the liver uptake–to–voxel ratio was then quantitatively calculated.

Liver blood flow measurement

On day 30 post-surgery and following behavioral tests, anesthesia was induced in the rats with an intraperitoneal (IP) injection of ketamine (90 mg/kg BW) and xylazine (9 mg/kg BW); the liver was exposed through a midline cut. A laser Doppler blood flow measurement probe (Moor Instruments, UK) was positioned on the median lobe of the liver for measuring liver blood flow. The findings were documented as hepatic blood flow normalized to perfusion units (27).

Cerebrospinal fluid (CSF) sampling

Following the analysis of liver blood flow, CSF was collected via a technique detailed previously (5). First, the incision site was sterilized. The rat's head was positioned at a 135° angle for CSF collection. Following collection, the samples underwent centrifugation and were then preserved at -80 °C for later ammonia detection using an assay kit.

Tissue preparation

After isolating the CSF, the ascites volume was ascertained. The ascites formation was categorized into the following scores: 0 indicates absence of peritoneal fluid, a score of 1 denotes mild peritoneal fluid accumulation, defined as lower than 3 ml, a score of 2 reflects moderate ascites, characterized by fluid accumulation ranging from 3 to 6 ml, and 3 represents severe ascites, defined as fluid accumulation exceeding 6 ml (28). Thereafter, the liver was excised and promptly weighed. Samples of the liver were

then preserved in formalin for histopathology assessments. Hematoxylin and eosin (H&E) staining was applied to the samples for examination. Finally, Masson's trichrome staining was utilized to detect liver pathology and appraise fibrotic scores (29).

Blood and CSF biochemistry markers

On day 30 post-surgery, blood obtained through cardiac puncture was centrifuged, after which the resulting plasma was preserved at −80 °C for the following examination. The levels of alanine aminotransferase (ALT), alkaline phosphatase (ALP), aspartate aminotransferase (AST), direct bilirubin, total bilirubin, and albumin in the serum were ascertained using a regular kit (Pars Azmun Co, Iran). Levels of serum and CSF ammonia were measured using an ammonia assay kit (Ziest Chem Diagnostics, Iran). All parameters were analyzed via an auto-analyzer (BT-1500; Biotecnica Instruments, Italy).

Hepatic and frontal cortex TNF-α, IL-6, and ROS levels, plus serum LPS, liver hydroxyproline, and Ileum occludin levels

Once blood and CSF were collected, the rats were beheaded, with their brains extracted. The brain structures were immediately dissected. The frontal cortex, liver tissue, and ileum tissue were isolated and kept at −80 °C for subsequent analysis. Hepatic and frontal cortex levels of TNF-α (Cat No: RTA00, R&D, USA), IL-6 (Cat No: CSB-E04640r), and ROS (Cat No: SL1189Ra) were quantified using ELISA kits following the manufacturer's directions (Quantikine ELISA detection kit, Taiwan). Further, serum LPS (Cat No: RK04263, ABclonal, USA), liver hydroxyproline (Cat No: MBS2000315, MyBioSource, San Diego, CA, USA), and Ileum occludin (Cat No: ER1906, Finetest, China) levels were measured via ELISA to further appraise inflammatory and barrier function markers.

Hematological cell count

One milliliter of blood mixed with EDTA was utilized for the blood cell quantification, which was conducted by an automated blood cell counter (Sysmex cell counter).

Western blot analysis

The western blot analyses were undertaken following a formerly established protocol (30). Anti-BDNF (Cat No: ab108319, Abcam) was used along with Anti-TLR4 (Cat No: ab217274), Anti-NF-kB p65 (Cat No: ab76302), Anti-VEGF (Cat No: ab46154), and anti-β actin-loading control antibodies (Cat No: ab8227). Protein bands were analyzed through densitometry with the aid of Gel Analyzer Version 2010a software.

Statistical analysis

Quantitative variables that followed a normal distribution were reported as Mean ± SEM. Statistical analyses were performed using one-way analysis of variance (ANOVA) and post hoc Tukey's test in SPSS version 27, with normality of the data assessed using the Shapiro-Wilk test. *P*-values less than 0.05 were deemed significant for all data sets.

Results

Effect of probiotic LGG and sorafenib combination on liver mass and peritoneal ascites

The results of the one-way ANOVA indicated a significant difference among the groups in liver mass, [F(4, 33) = 13.2, *P*=0.000]. The BDL (*P*<0.001), PRO (*P*<0.001), and SOR (*P*<0.01) groups significantly increased liver mass when compared to the sham group (Figure 1A), but the PRO+SOR group did not present a significant difference compared to the sham group. In the SOR group, liver mass significantly diminished compared to the BDL (*P*<0.01) group. In the PRO+SOR group, liver mass significantly declined compared to the BDL and PRO groups (*P*<0.001, *P*<0.01, respectively). All groups except the sham group

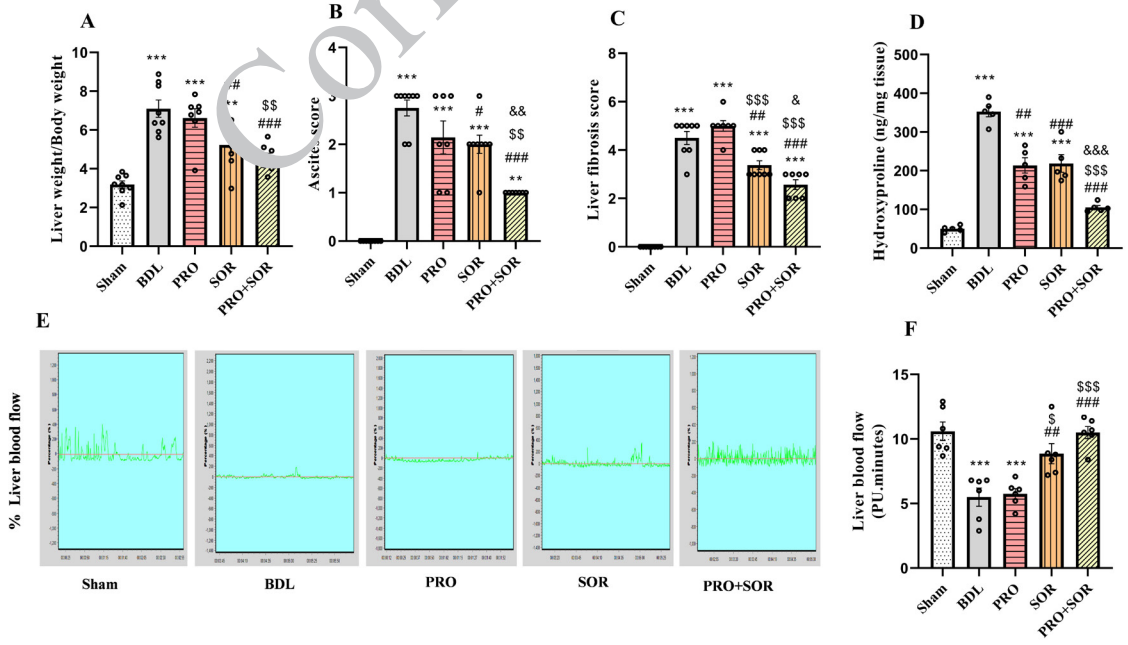

Figure1. Liver mass, ascites formation, liver fibrosis score, hydroxylproline, and liver blood flow in various rat experimental groups
A) Ratio of liver weight to body weight. B) Ascites score. C) Liver fibrosis score. D) Liver hydroxyproline. E) Percentage chart of liver blood flow. F) Liver blood flow. All values are presented as Mean ± SEM. BDL: bile duct ligation; SOR: sorafenib; PRO: probiotic LGG; PRO+SOR: probiotic LGG + sorafenib. **P*<0.05, ***P*<0.01, ****P*<0.001 significant vs sham group. # *P*<0.05, ##*P*<0.01, ### *P*<0.001 significant vs BDL group. $ *P*<0.05, $$*P*<0.01, $$$*P*<0.001 significant vs PRO group. &*P*<0.05, &&*P*<0.01, &&&*P*<0.001 significant vs SOR group.

produced peritoneal ascites (Figure 1B). The findings of the one-way ANOVA demonstrated a significant difference among the groups in ascites score, [F(4, 33) = 17.0, *P*=0.000]. The score of ascites was significantly reduced in the SOR group compared with the sham and BDL groups (*P*<0.001 and *P*<0.05, respectively). In the PRO+SOR group, the score of ascites significantly dropped compared with the sham (*P*<0.01), BDL (*P*<0.001), PRO (*P*<0.01), and, interestingly, SOR (*P*<0.01) groups.

Impact of combining probiotic LGG with sorafenib intake on liver fibrosis

The results of the one-way ANOVA exhibited a significant difference among the groups in liver fibrosis score, [F(4, 29) = 54.71, *P*=0.000]. In a double-blinded manner, the liver fibrosis score in all groups was significantly greater than in the sham group (Figure 1C, *P*<0.001 for all groups), reflecting biliary duct expansion and inflammation in the BDL rats. Current observations revealed that in the SOR group, fibrosis score significantly fell compared to the BDL and PRO groups (*P*<0.01, *P*<0.001, respectively). In the PRO+SOR group, the fibrosis score significantly diminished compared to the BDL, PRO, and SOR groups (*P*<0.001, *P*<0.001, *P*<0.05, respectively). The results of the one-way ANOVA showed a significant difference among the groups in the liver hydroxyproline levels, [F(4, 20) = 60.9, 4 *P*=0.000]. Liver hydroxyproline measurement presented a significant rise in the BDL, PRO, and SOR groups compared to the sham group (Figure1D, *P*<0.001, for all groups). Levels of liver hydroxyproline in the PRO+SOR group significantly dropped compared to the PRO and SOR group alone (*P*<0.001, for both groups).

Liver blood flow was enhanced by combining sorafenib with probiotic LGG

The percentage chart of liver blood flow is depicted in Figure 1E, indicating that the combination of probiotic LGG and sorafenib enhanced liver blood flow. The results of the one-way ANOVA demonstrated a significant difference among the groups in the liver blood flow, [F(4, 25) = 14.71, *P*=0.000]. The liver blood flow in the BDL and PRO groups revealed a decline in comparison to the sham group (Figure 1F, *P*<0.001 for both groups). In the SOR group, liver blood flow was significantly boosted compared with the BDL (*P*<0.01) and PRO groups (*P*<0.05). In the PRO+SOR group, liver blood flow significantly grew compared with the BDL and PRO groups (*P*<0.001, for both groups).

Impact of sorafenib with probiotic LGG intake on liver and brain injury induced by BDL

BDL primarily results in significant hepatocellular damage and progression of liver fibrosis. Levels of biochemical markers for liver fibrosis in both serum and liver tissue presented a significant growth in the BDL group when compared to the sham group (Figure 2, A-B, and Table 1). H&E and Masson's trichrome staining were used to ascertain hepatic fibrosis and collagen disposition. In the sham group, normal liver parenchyma with normal bile duct structure was observed. Post-BDL, the tissue was disorganized with collagen disposition, bile duct proliferation, feathery changes, and inflammation. Usage of sorafenib also improved this disorder; sorafenib with probiotic LGG consumption presented

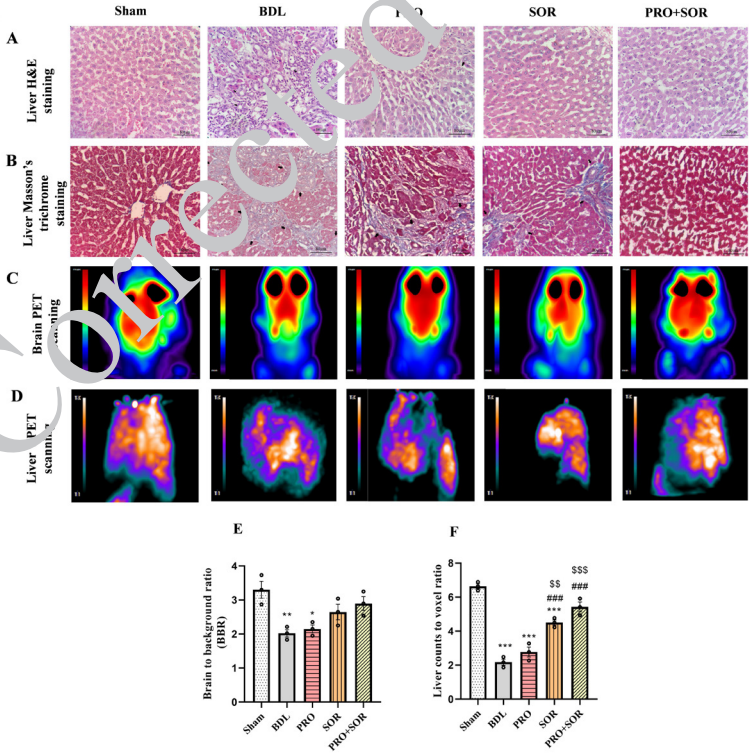

Figure 2. Histological analysis of liver tissue and small animal PET brain and SPECT liver images for rats in various experimental groups
(A-B) Liver pathological changes were detected by H&E and Masson's trichrome staining (×200). The presence of arrows in the images suggests the following bile duct changes: necrosis, fibrosis, inflammation, and collagen deposition. C) Small animal PET brain images. D) SPECT liver images. E) Brain-to-background ratio. F) Liver counts-to-voxel ratio. The intensity of the red color that appears is directly proportional to glucose uptake (18FDG) in rat brains, as indicated by the scale bar. The intensity of the white color that appears is directly proportional to radioactive compound 99m Tc-phytate in rat livers, as indicated by the scale bar. BDL: bile duct ligation; SOR: sorafenib; PRO: probiotic LGG; PRO+SOR: probiotic LGG + sorafenib. **P*<0.05, ***P*<0.01, ****P*<0.001 significant vs sham group. # *P*<0.05, ##*P*<0.01, ### *P*<0.001 significant vs BDL group. $ *P*<0.05, $$*P*<0.01, $$$*P*<0.001 significant vs PRO group.

Table 1. Serum biochemical analysis in different rat experimental groups

	Sham	BDL	PRO	SOR	PRO+SOR
AST (U/l)	187.0±32.55	780.66±36.37***	631.16±87.41***	391.2±25.82###$	182.0±16.93###$$$&
ALT (U/l)	56.80±6.76	205.8±16.39**	248.00±27.17***	206.0±43.46**	95.00±13.83#$$&
ALP (U/l)	258.2±20.23	1184±79.04***	840.6±125.6**	1040±94.19***	783.8±113.3**#
Direct bilirubin (mg/dl)	0.25±0.03	5.60±0.41***	5.82±0.55***	5.22±1.09***	1.00±0.65###$$$&
Total bilirubin (mg/dl)	0.5667±0.04	11.02±0.72***	11.64±1.10***	10.46±2.17***	2.060±1.31###$$$&&&
Albumin (g/dl)	2.214±0.04	1.917±0.04	1.760±0.05	1.49±0.25**	2.167±0.09&&
Ammonia (µmol/l)	179.92±7.21	340.38±26.31***	322.05±20.04***	269.34±12.61*	191.10±10.89###$$$&
CSF Ammonia (µmol/l)	25.20±1.74	91.40±3.20***	54.80±12.53***###	46.20±4.91***###	29.00±3.53###$$$&&

Note: All values are expressed as Mean ± SEM. BDL: bile duct ligation; SOR: sorafenib; PRO: probiotic; PRO+SOR: Probitic + Sorafenib. *P<0.05, **P<0.01, ***P<0.001 significant vs sham group. # P<0.05, ##P<0.01, ### P<0.001 significant vs BDL group. $ P<0.05, $$$P$<0.01, $$$$P$<0.001 significant vs PRO group. & P<0.05, && P<0.01, &&& P<0.001 significant vs SOR group

significant improvements in the liver parenchyma.

Following induction of BDL and HE, PET scans were utilized for measuring brain injury and SPECT scans for specifying liver injury damage (Figure 2, C-F). PET scan figures are presented in Figure 2C. Qualitative analysis of the PET scan Figures indicated that absorption of 18FDG diminished in the BDL group compared to the sham group, showcasing brain injury. Higher absorption of 18FDG was observed in the PRO+SOR group in comparison to the BDL group.

SPECT scan figures are outlined in Figure 2D. Qualitative analysis in SPECT scans demonstrated that absorption of 99mTc-Phytate in the liver declined in the BDL group compared to the sham group. Observation of 99mTc-Phytate absorption in the liver revealed that both the SOR and PRO+SOR groups had higher densities of 99mTc-Phytate compared to the BDL group.

The results of the one-way ANOVA indicated a significant difference among the groups in the BBR, [F(4, 10) = 7.71, P=0.004]. The quantitative data for PETs are exhibited in Figure 2E, showing that the BBR in the BDL and PRO groups diminished compared to the sham group (Figure 2E, P<0.01 and P<0.05, respectively) and presented brain dysfunction consistent with HE in these groups, thereby confirming the presence of HE.

The results of the one-way ANOVA exhibited a significant difference among the groups in the liver counts to voxel ratio, [F(4, 10) = 70.16, P=0.000]. The quantitative data for SPECTs are illustrated in Figure 2F, indicating that the liver counts to voxel ratio in the BDL, PRO, and SOR groups (P<0.001 for all groups) were significantly lower compared to the sham groups, signaling liver fibrosis after BDL. The liver counts to voxel ratio in the SOR and PRO+SOR groups was significantly higher than in the BDL (P<0.001 for both groups) and PRO groups (P<0.01 and P<0.001, respectively).

Effect of combining sorafenib with probiotic LGG on blood cells

The results of the one-way ANOVA demonstrated a significant difference among the groups in white blood cell (WBC) counts, [F(4, 25) = 10.42, P=0.000]. A notable rise in WBC count was noted in the BDL group when compared to the sham group (Figure 3A, P<0.001). WBCs in the SOR and PRO+SOR groups significantly dropped compared with the BDL group (P<0.05 and P<0.01, respectively).

The results of the one-way ANOVA indicated a significant difference among the groups in the red blood cells (RBC), [F(4, 23) = 6.09, P=0.001]. In the BDL and PRO groups, RBC significantly diminished compared with the sham group (Figure 3B, P<0.001 and P<0.05, respectively). RBCs in the SOR group were significantly augmented compared with the BDL group (P<0.01). In the PRO+SOR group, RBCs significantly rose compared with the BDL and PRO groups (P<0.001 and P<0.05, respectively).

Impact of combining probiotic LGG with sorafenib on Liver Function parameters

The results of the one-way ANOVA presented a significant difference among the groups in the ALT [F(4,

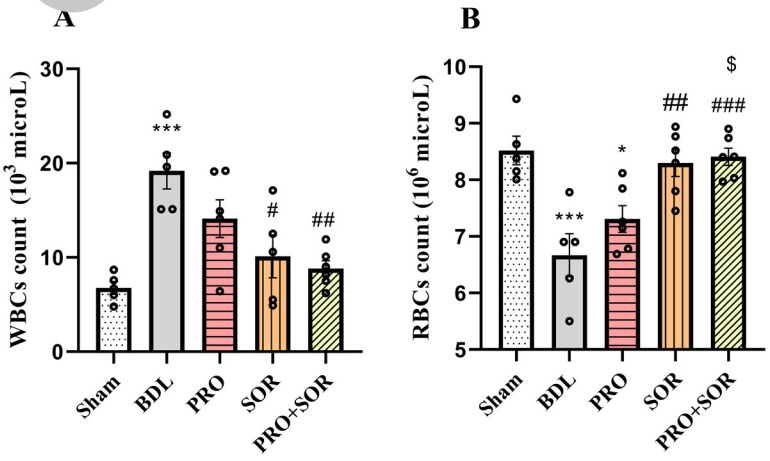

Figure 3. A) WBC count in different experimental groups. (B) RBC count in different experimental groups
All values are presented as Mean ± SEM. BDL: bile duct ligation; SOR: sorafenib; PRO: probiotic LGG; PRO+SOR: probiotic LGG + sorafenib. *P<0.05, **P<0.01, ***P<0.001 significant vs sham group. # P<0.05 significant vs BDL group. $ P<0.05, $$$P$<0.01 significant vs PRO group.

20) = 10.69, *P*=0.000], AST [F(4, 24) = 31.80, *P*=0.000], ALP [F(4, 21) = 14.54, *P*=0.000], serum ammonia [F(4, 22) = 17.17, *P*=0.000], CSF ammonia [F(4, 20) = 67.32, *P*=0.000], direct bilirubin [F(4, 21) = 19.73, *P*=0.000], total bilirubin [F(4, 21) = 19.81, *P*=0.000, Albumin [F(4, 28) = 5.08, *P*=0.003]. The BDL group presented a significant growth in serum levels of biochemical markers [ALT (*P*<0.01), AST (*P*<0.001), ALP (*P*<0.001), serum ammonia (*P*<0.001), CSF ammonia (*P*<0.001), direct bilirubin (*P*<0.001), and total bilirubin (*P*<0.001)] when compared to the sham group, suggesting successful development of liver failure in BDL-induced rats (Table 1). When BDL rats were administered a combination of sorafenib and probiotic LGG, significant reductions in the liver enzyme levels of ALT and AST were noted compared to the SOR group alone (*P*<0.05, for both groups), suggesting the beneficial impact of consuming this combination on liver health. Our findings revealed that the combination of probiotic LGG and sorafenib led to a significant drop in serum levels of total bilirubin and direct bilirubin compared to the SOR group alone (*P*<0.001, *P*<0.01, respectively).

CSF ammonia levels in the BDL, PRO, and SOR groups were significantly elevated compared to the sham group (*P*<0.001, *P*<0.001, *P*<0.01, respectively). CSF ammonia levels in the PRO, SOR, and PRO+SOR groups significantly declined compared to the BDL group (*P*<0.001, for all groups). CSF ammonia levels in the PRO+SOR group significantly diminished compared to the SOR group (*P*<0.01).

Serum levels of Ammonia in BDL, PRO, and SOR groups significantly rose compared to the sham group (*P*<0.001, *P*<0.001, *P*<0.05, respectively). Serum ammonia levels in the PRO+SOR group significantly dropped compared to the SOR group (*P*<0.05).

Consuming probiotic LGG along with sorafenib led to a reduction in inflammatory markers and oxidative stress within the liver

The results of the one-way ANOVA exhibited a significant difference among the groups in the levels of IL-6 [F(4, 15) = 39.45, *P*=0.000] and TNF-α [F(4, 15) = 52.32, *P*=0.000].

The IL-6 and TNF-α levels in the liver tissue of the BDL group showed a significant increase when compared to those in the sham group (Figure 4, A-B and *P*<0.001). The levels of IL-6 and TNF-α of liver tissue in the PRO+SOR group significantly diminished compared to the BDL and SOR groups (*P*<0.001, *P*<0.05, respectively). Thus, the consumption of sorafenib with probiotic LGG significantly alleviated the inflammation in the liver tissue.

The results of the one-way ANOVA showed a significant difference among the groups in the levels of Liver ROS [F(4, 15) = 37.35, *P*=0.000]. The levels of Liver ROS levels in the

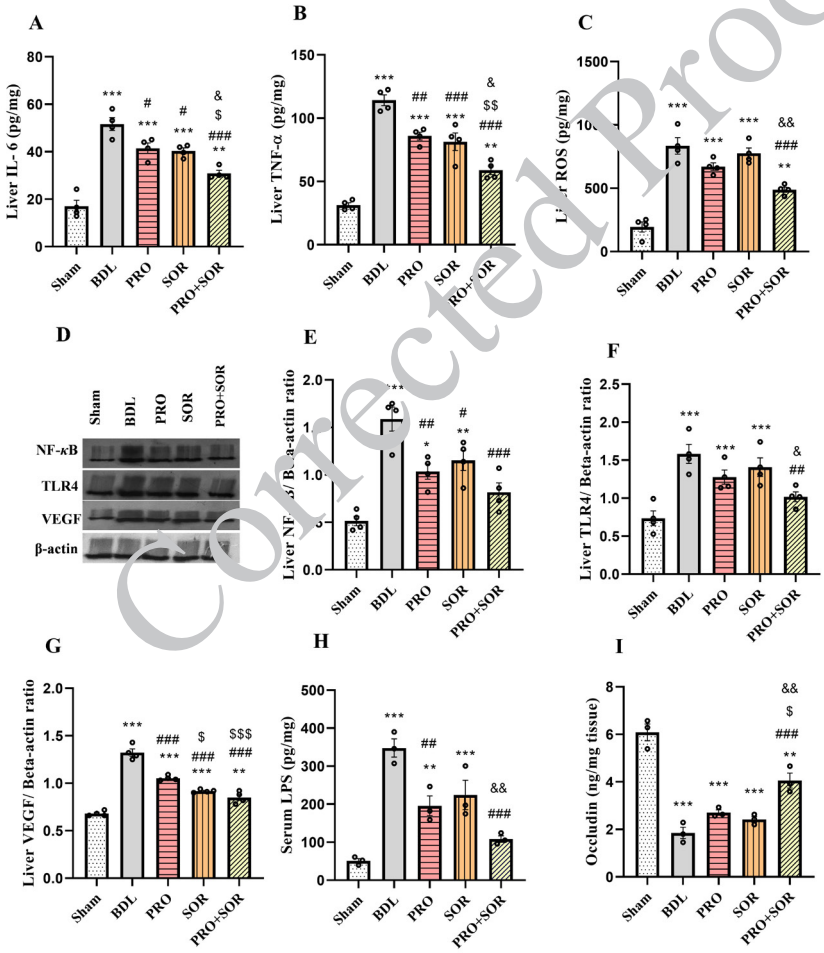

Figure 4. Liver tissue inflammatory markers, oxidative stress, expression of the TLR4/NF-κB signaling pathway, VEGF, serum LPS and ileum occludin in different rat experimental groups

A) Liver tissue levels of IL-6 (pg/mg). B) Liver tissue levels of TNF-α (pg/mg). C) Liver tissue levels of ROS (pg/mg). D) Western blot analysis of NF-κB, TLR4, and VEGF. E) NF-κB protein levels (liver NF-κB/ beta-actin ratio). F) TLR4 protein levels (liver TLR4/beta-actin ratio). G) VEGF protein levels (liver VEGF/ beta-actin ratio). H) Serum LPS levels (pg/mg). I) Ileum tissue levels of Occludin (pg/mg tissue). All values are presented as Mean ± SEM. BDL: bile duct ligation; SOR: sorafenib; PRO: probiotic LGG; PRO+SOR: probiotic LGG + sorafenib. **P*<0.05, ***P*<0.01, ****P*<0.001 significant vs sham group. # *P*<0.05, ##*P*<0.01, ### *P*<0.001 significant vs BDL group. $ *P*<0.05, $$*P*<0.01, $$$*P*<0.001 significant vs PRO group. &*P*<0.05, &&*P*<0.01, &&&*P*<0.001 significant vs SOR group.

BDL, PRO, SOR (P<0.001 for all groups), and PRO+SOR (P<0.01) groups significantly rose compared to the sham group (Figure 4C). Liver ROS levels in the PRO+SOR group significantly fell compared to the BDL and SOR groups (P<0.001, P<0.01, respectively). Co-administration of sorafenib with probiotic LGG, as opposed to sorafenib alone, led to lowered ROS levels in the liver.

Impact of consuming probiotic LGG with sorafenib on the activation of TLR4/NF-κB signal pathway

The TLR4/NF-κB signaling pathway can potentially enhance and intensify the inflammatory response during inflammation. Levels of TLR4/NF-κB proteins were appraised using western blot analysis (Figure 4, D-F). The results of the one-way ANOVA demonstrated a significant difference among the groups in the levels of NF-κB [F(4, 15) = 17.23, P=0.000] and TLR4 [F(4, 15) = 16.39, P=0.000].

The levels of the liver NF-κB in the BDL, PRO, and SOR groups were significantly heightened compared to the sham group (Figure 4E, P<0.001, P<0.05, and P<0.01, respectively). In the PRO, SOR, and PRO+SOR groups, the levels of NF-κB in liver tissue significantly diminished compared to the BDL group (P<0.01, P<0.05, and P<0.001, respectively).

The protein levels of TLR4 significantly rose in the BDL, PRO, and SOR groups compared with the sham group (Figure 4F, P<0.001 for all groups). In the PRO+SOR group, levels of TLR4 in liver tissue significantly fell compared to both the BDL and SOR groups (P<0.01 and P<0.05, respectively). Hence, the combined usage of sorafenib and probiotic LGG leads to a greater reduction in TLR4 protein levels compared to the use of sorafenib alone.

According to the data, levels of the TLR4 and NF-κB proteins in the BDL group were significantly diminished by sorafenib with probiotic LGG cotreatment (P<0.01, P<0.001, respectively).

Effect of probiotic LGG and sorafenib Combination on angiogenesis

The results of the one-way ANOVA indicated a significant difference among the groups in the levels of VEGF [F(4, 15) = 98.10, P=0.000]. Levels of VEGF protein were ascertained using western blot analysis (Figure 4, D and G). Analysis of data revealed that the liver VEGF levels in the BDL (P<0.001), PRO (P<0.001), SOR (P<0.001), and PRO+SOR (P<0.01) groups significantly grew compared to the sham group (Figure 4G). In the PRO, SOR, and PRO+SOR groups (P<0.001 for all groups), liver VEGF levels significantly declined compared to the BDL group.

Beneficial effects of combining probiotic LGG with sorafenib on serum endotoxin (LPS) levels and intestinal barrier function

The results of the one-way ANOVA exhibited a significant difference among the groups in the levels of Serum LPS [F(4, 10) = 28.93, P=0.000] and Ileum occludin [F(4, 10) = 45.84, P=0.000]. Serum LPS levels were significantly elevated in the BDL, PRO, and SOR groups compared to the sham group (Figure 4H, P<0.001, P<0.01, P<0.001, respectively). Nevertheless, in the PRO+SOR group, serum LPS levels were significantly lowered compared to the SOR group alone (P<0.01). Ileum occludin levels significantly dropped in the BDL, PRO, and SOR groups compared to the sham group (Figure 4I, P<0.001 for all groups). In the PRO+SOR group, occludin levels differed significantly from the SOR group (P<0.01) and resembled those of the sham group.

These results suggest that the combination of sorafenib and LGG would enhance ileum barrier integrity by increasing occludin expression, which consequently leads to a decline in LPS levels in the blood.

Sorafenib in combination with probiotic LGG mitigates memory impairment

Memory and learning were appraised using a NORT and a passive avoidance test (Figure 5A-B). The results of the one-way ANOVA demonstrated a significant difference among the groups in the time of step-through In the passive avoidance test [F(4, 33) = 16.17, P=0.000]. In the passive avoidance test, the time it took for the animals in the BDL, PRO, and SOR groups to enter the dark compartment was

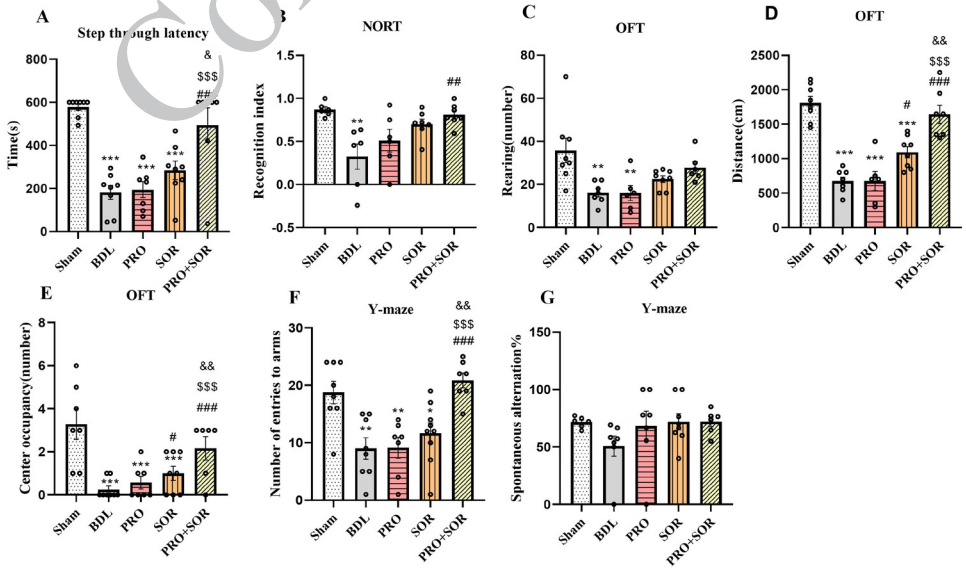

Figure 5. Step-through latency in the shuttle box test, short-term memory performance in the novel object recognition test, measurement of rearing, distance moved, center occupancy in the open field test, number of entries, and percentage of spontaneous alternations in the Y-maze test among rat experimental groups A) Time of step-through latency. B) RI in the novel object recognition test. C) Number of rearings in rats. D) Total distance moved in the open field test. E) Number of entries into the center of the box. F) Total number of entries. G) Percentage of spontaneous alternations. All values are presented as Mean ± SEM. BDL: bile duct ligation; SOR: sorafenib; PRO: probiotic LGG; PRO+SOR: probiotic LGG + sorafenib. *P<0.05, **P<0.01, ***P<0.001 significant vs sham group. # P<0.05, ##P<0.01, ### P<0.001 significant vs BDL group. $ P<0.05, $$$P$<0.01, $$$$P$<0.001 significant vs PRO group. &P<0.05, &&P<0.01, &&&P<0.001 significant vs SOR group.

significantly shorter compared to the sham group (Figure 5A, $P<0.001$ for all groups). This reflects a deficit in learning and memory in BDL. The time of step-through latency in the PRO+SOR group was markedly augmented compared to the BDL, PRO, and SOR groups ($P<0.001$, $P<0.001$, $P<0.05$, respectively).

The results of the one-way ANOVA showed a significant difference among the groups in the RI of the the NORT[$F(4, 27) = 5.79$, $P=0.001$]. In the NORT, the RI of the BDL group significantly declined compared to the sham group (Figure 5B, $P<0.01$). The RI in the PRO+SOR group was markedly enhanced compared to the BDL group ($P<0.01$).

Impact of consuming sorafenib with probiotic LGG on performance in open field and Y-maze tests

The results of the one-way ANOVA indicated a significant difference among the groups in the rearing behavior [$F(4, 30) = 5.69$, $P=0.001$].

The BDL and PRO groups exhibited a significant decrement in rearing behaviors when compared to the sham group (Figure 5C, $P<0.01$ for both groups). In contrast, the SOR and PRO+SOR groups did not present a significant variance from the sham group in this aspect.

The results of the one-way ANOVA demonstrated a significant difference among the groups in the distance traveled [$F(4, 32) = 28.18$, $P=0.000$]. The BDL, PRO, and SOR groups revealed a significant reduction in the distance traveled compared to the sham group (Figure 5D, $P<0.001$ for all groups). The distance moved in the SOR group significantly grew compared to the BDL group ($P<0.05$). General locomotor activity (distance) in the PRO+SOR group was significantly augmented compared to the BDL, PRO, and SOR groups ($P<0.001$, $P<0.001$, $P<0.01$, respectively), showing better locomotor activity in the PRO+SOR group.

The results of the one-way ANOVA indicated a significant difference among the groups in the center occupancy [$F(4, 31) = 8.42$, $P=0.000$]. In the BDL, PRO, and SOR groups, center occupancy significantly diminished compared to the sham group (Figure 5E, $P<0.001$ for all groups). Center occupancy was significantly enhanced in the SOR group compared to the BDL group ($P<0.05$). In the PRO+SOR group center, occupancy significantly rose compared to the BDL, PRO, and SOR groups ($P<0.001$, $P<0.001$, $P<0.01$, respectively).

The results of the one-way ANOVA showed a significant difference among the groups in the number of entries into arms [$F(4, 34) = 10.16$, $P=0.000$]. In the PRO+SOR group, the number of entries into arms significantly rose compared to the BDL, PRO, and SOR groups (Figure 5F, $P<0.01$, $P<0.01$, $P<0.05$, respectively), reflecting hyperactivity. Whereas the BDL group exhibited a lower frequency of alternations compared with the other groups, this difference was not statistically significant (Figure 5G).

Consuming probiotic LGG along with sorafenib led to a reduction of inflammatory markers and oxidative stress within the brain

The results of the one-way ANOVA exhibited a significant difference among the groups in the levels of Frontal cortex IL-6 [$F(4, 15) = 72.66$, $P=0.000$]. Frontal cortex IL-6 levels in the BDL ($P<0.001$), PRO ($P<0.001$), SOR ($P<0.01$), and PRO+SOR ($P<0.05$) groups were significantly heightened compared to the sham group (Figure 6A). Frontal cortex IL-6 levels in the PRO, SOR, and PRO+SOR groups significantly lessened compared to the BDL group ($P<0.001$ for all groups). IL-6 levels of the frontal cortex in the SOR and PRO+SOR groups significantly dropped compared to the PRO group ($P<0.01$, $P<0.001$, respectively).

The results of the one-way ANOVA illustrated a significant difference among the groups in the levels of Frontal cortex

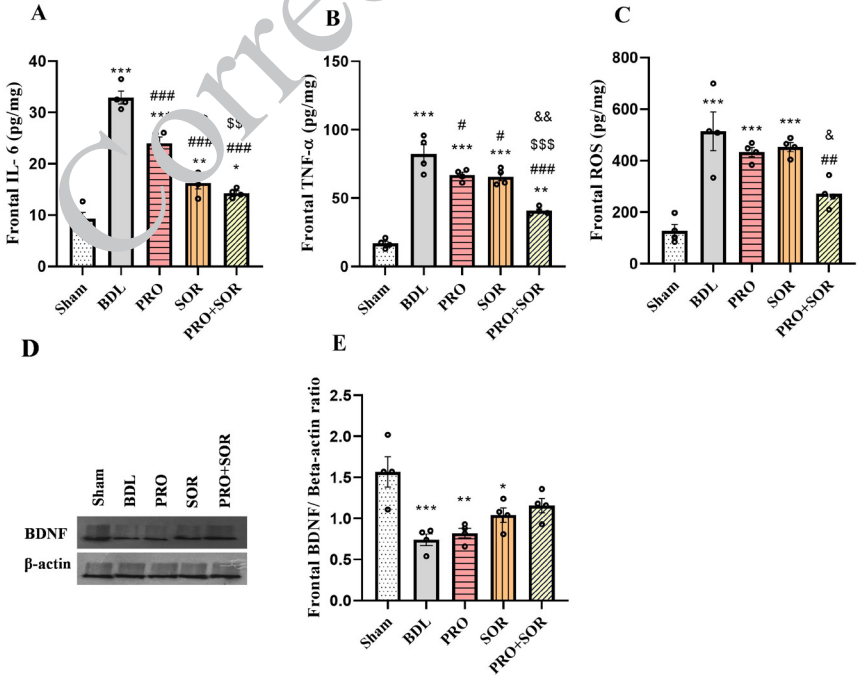

Figure 6. Frontal cortex tissue inflammatory markers, oxidative stress, and frontal cortex BDNF in different rat experimental groups
A) Frontal cortex tissue levels of IL-6 (pg/mg). B) Frontal cortex tissue levels of TNF-α (pg/mg). C) Frontal cortex tissue levels of ROS (pg/mg). D) Western blot analysis of BDNF. E) Measurement of frontal cortex BDNF (frontal cortex BDNF/ beta-actin ratio). All values are presented as Mean ± SEM. BDL: bile duct ligation; SOR: sorafenib; PRO: probiotic LGG; PRO+SOR: probiotic LGG + sorafenib. *$P<0.05$, **$P<0.01$, ***$P<0.001$ significant vs sham group. # $P<0.05$, ##$P<0.01$, ###$P<0.001$ significant vs BDL group. $ $P<0.05$, $$$P<0.01$, $$$$P<0.001$ significant vs PRO group. &$P<0.05$, &&$P<0.01$ significant vs SOR group.

TNF-α [F(4, 15) = 53.84, *P*=0.000]. Frontal cortex TNF-α levels in the BDL, PRO, SOR (*P*<0.001 for all groups), and PRO+SOR (*P*<0.01) groups markedly rose compared to the sham group (Figure 6B). In the PRO+SOR group, frontal cortex TNF-α levels significantly declined compared to the BDL, PRO, and SOR groups (*P*<0.001, *P*<0.001, *P*<0.01, respectively). Thus, the consumption of sorafenib with probiotic LGG significantly mitigated the inflammation in the frontal cortex tissue. Frontal cortex ROS levels in the BDL, PRO, and SOR groups were markedly elevated compared to the sham group (Figure 6C, *P*<0.001 for all groups). The results of the one-way ANOVA presented a significant difference among the groups in the levels of Frontal cortex ROS [F(4, 15) = 16.39, *P*=0.000]. Frontal cortex ROS levels in the PRO+SOR group significantly dropped compared to the BDL and SOR groups (*P*<0.01, *P*<0.05, respectively).

Impact of sorafenib with probiotic LGG consumption on frontal cortex BDNF levels

The results of the one-way ANOVA indicated a significant difference among the groups in the Levels of BDNF [F(4, 15) = 9.22, *P*=0.000]. Levels of BDNF protein were appraised using western blot analysis (Figure 6, D-E).

Frontal cortex BDNF levels in the BDL, PRO, and SOR groups significantly fell compared to the sham group (Figure 6E, *P*<0.001, *P*<0.01, *P*<0.05, respectively). The BDNF protein level was not altered in the PRO+SOR group compared to the sham group.

Discussion

The current research explored the effects of combining sorafenib and the probiotic LGG on liver fibrosis and HE in rats after BDL. A comprehensive assessment included histological parameters, SPECT scans, biochemical markers, hydroxyproline levels, blood flow, angiogenesis, oxidative stress indicators, and inflammatory pathways in the liver, as well as PET scans, BDNF levels, cognition tests, and motor disturbances in the frontal cortex and ileum occludin levels. According to the findings, administering LGG alongside sorafenib led to better outcomes for liver fibrosis and HE compared to sorafenib alone.

Sorafenib has been studied at doses between 20 and 80 milligrams in various BDL model studies (31). In our previous work, sorafenib was administered at doses of 30 and 60 mg/kg (27). In the current study, a lower dose of 20 mg/kg was employed to mitigate potential side effects (9, 32). This dosing strategy aligns with clinical scenario where the drug's effectiveness is hindered by its tolerability in patients with liver diseases. The findings of the present study confirmed that the modulation of the gastrointestinal-liver axis using LGG can significantly boost the effectiveness of a low-dose sorafenib. This indicates a promising way forward beyond dose escalation and towards a 'combination-based' model. Further dose-response relationship-based research is definitely recommended.

BDL model causes cholestasis through bile duct obstruction, resulting in inflammation and damage to cells and eventually liver fibrosis through fibrogenic activation and accumulation of ECM. In this study, the model was mainly utilized to induce liver fibrosis and not to examine cholestasis itself, as it has been found to effectively model some of the main characteristics of liver pathology, such as inflammation, myofibroblast activation, and fibrosis progression. Even though it presents an obstructive model of fibrosis, it can still be applied for inspecting mechanisms of liver fibrosis, portal hypertension, and the gut-liver axis. Other chronic liver disease models, such as MASH or alcoholic liver disease, should be validated to expand the scope of these findings (33).

In chronic liver disease, toxins including ammonia, bilirubin, and inflammatory factors accumulate in the blood, negatively impacting the brain and resulting in a neuropsychiatric condition known as HE (34). Several studies have indicated that sorafenib can attenuate liver fibrosis. These findings support its potential use in early-stage liver fibrosis models, though it is not yet a standard clinical treatment for fibrosis (35). Sorafenib was selected owing to its known multi-kinase inhibitory effects, including its influence on pathways implicated in fibrosis progression, which we believe offer unique therapeutic potential. While we acknowledge the existence of other antifibrotic candidates, sorafenib's established clinical use and safety profile offer a valuable foundation for repurposing in liver fibrosis. Nevertheless, it is linked to drug resistance and adverse effects (10). Since the microbiota of the intestines is vital in regulating the body's response to drugs and the emergence of adverse effects (4), alteration of gut microbiota and the presence of endotoxemia play substantial roles in furthering the progression of long-term liver conditions and the onset of liver cancer. Probiotics offer various benefits through multiple mechanisms, including direct modulation of gut microbiota as well as indirect effects such as immune modulation, diminished bacterial translocation, anti-inflammatory activities, and augmented intestinal barrier integrity (36).

Current findings support previous research, indicating that BDL leads to liver damage (37). The PRO+SOR group presented higher 99mTc-Phytate absorption and a lower fibrosis score than the BDL group. Further, this group showed lowered hydroxyproline levels relative to the SOR group alone, indicating a more pronounced improvement in liver fibrosis. The study found that In the PRO group, there was a significant decline in the level of hydroxyproline rather than BDL group suggesting that the improvement of liver fibrosis is due to probiotic effect. Several studies have reported that sorafenib can lower ascite levels (38) and restore liver enzyme balance (19). Several studies have found that probiotics such as LGG reduce levels of ALP, AST, ALT, direct bilirubin, and total bilirubin, resulting in the alleviation of liver cell damage (39). Current findings support previous studies, suggesting that when sorafenib is combined with the LGG, liver fibrosis improves compared to sorafenib alone, possibly due to a synergistic or additive effect. The study noted that the combination of sorafenib and LGG significantly elevates albumin levels while lowering liver enzyme concentration. BDL procedure elevated both direct and total bilirubin levels; however, the PRO+SOR group showed significant reductions in these bilirubin levels compared to other groups, thereby enhancing liver function. Numerous studies have indicated that BDL raises ammonia levels, resulting in HE (4). In the current study, the BDL group showed elevated ammonia levels, while sorafenib effectively diminished these levels. The combination of LGG with sorafenib produced even better results in lessening ammonia levels. Nevertheless, LGG alone was ineffective on lowering ammonia levels, reflecting a synergistic or effect when used with sorafenib. Although the PET/SPECT data

(brain-to-background ratio, liver counts) did not show significant differences between SOR and PRO+SOR groups, this aligns with our expectation, since these scans primarily served to validate disease progression rather than quantify treatment efficacy. The key improvements in fibrosis and HE were instead demonstrated through other tests.

In accordance with other reports, the BDL model exhibited a higher number of WBCs (40) and reduced RBCs (41). Consistent with previous studies, sorafenib treatment led to a reduced count of WBCs (42). Unlike previous research (43), the current study found that sorafenib does not lower but rather raise the number of RBCs, which may be due to the lower dose of the administered drug. PRO+SOR group did not show a significantly greater impact than sorafenib alone in altering these hematological parameters. While anemia has been cited as a common side effect of sorafenib treatment, as may be observed with the PRO + SOR group, its absence in the current treatment can be assigned to the dosage of the drug. Further studies include different dosage regimens of the drug along with the potential reduction of its effects.

In line with other studies, the BDL model is characterized by impaired microvascular disruptions consisting of diminished blood flow (44). Sorafenib therapy has the potential to lower hepatic microvascular density and VEGF expression, resulting in enhanced liver blood circulation (27). In the current study, sorafenib administration significantly boosted hepatic blood flow. Blood flow increased even more following the treatment with sorafenib in combination with LGG. Further, numerous studies have indicated that angiogenesis is essential for the progression of liver fibrosis (45). VEGF is the most powerful factor promoting angiogenesis, most of anti-angiogenic treatments aim to block the VEGF signaling pathway (46). Sorafenib has been found to lower angiogenesis and portal hypertension (47) by blocking the signaling of VEGFR and PDGFR, which are essential for angiogenesis (48). We observed markedly elevated levels of VEGF within the hepatic region of BDL rats. Treatment with sorafenib alone and in combination with LGG resulted in lessened hepatic VEGF levels; however, no statistically meaningful difference was observed between the two treatments. In addition, in the PRO groups, VEGF level was significantly lower than in the BDL group. This aligns with the results of a 2022 study, showing that LGG lowered VEGF levels (49).

TLRs are critical in regulating inflammation, including injury and wound healing. The current study using the BDL model demonstrated a significant growth in inflammatory markers, enhanced hepatic function enzymes, and elevated fibrosis markers, in accordance with previous research (50). Notably, a significant elevation in inflammatory factors (IL-6 and TNF-α), TLR4/NF-κB axis activity, and heightened oxidative stress (ROS) levels were observed post-BDL (51). Sorafenib is a drug that inhibits the phosphorylation of tyrosine kinases triggered by LPS via TLR4, effectively lowering inflammatory factor expression, especially IL-6 and TNF-α, by blocking NF-κB activation. It also brings down TLR4 expression on macrophage membranes, contributing to its anti-inflammatory effects (52). In the present research, the consumption of sorafenib led to a significant decline in IL-6 and TNF-α, but it did not significantly lower TLR4 and NF-κB. Sorafenib's predominant anti-inflammatory actions in this model appear to be independent of substantial TLR4/NF-κB inhibition, while not ruling out possible modest contributions via this pathway, which might have been influenced by the current experimental conditions, including the timing and sensitivity of measurements. Nevertheless, the potential impact of sorafenib on the TLR4/NF-κB signaling should also be further explored.

Consistent with other studies, probiotics, particularly LGG, reduce lower inflammation and oxidative damage through the gut-liver connection. These effects are achieved by modulating TLR4/NF-κB signaling, leading to proinflammatory cytokines and a reduction in ALT levels (53-55). In the present study, we observed that when sorafenib is combined with the probiotic LGG, it not only lowers the levels of inflammatory cytokines (IL-6 and TNF-α) and ROS but also diminishes TLR4 and NF-κB expression. This suggests that the reduction in IL-6 and TNF-α levels is mediated by the inhibition of the TLR4/NF-κB axis in the PRO+SOR group. Further, intestinal integrity was ascertained by measuring ileum occludin levels. In the current study, the combination of LGG and SOR enhanced the intestinal barrier by boosting occludin expression, which was linked to a decline in serum LPS levels compared to SOR alone. These findings suggest that PRO+SOR improves ileum barrier function, thereby lowering LPS translocation and inhibiting the TLR4/NF-κB signaling pathway, ultimately mitigating inflammation. Our present data suggest that LGG improves intestinal barrier integrity and diminishes systemic endotoxemia, which indirectly dampens TLR4/NF-κB signaling. Further studies are required to address the direct cellular and molecular interactions by which LGG modulates immune and inflammatory pathways (56). In the PRO group, we observed that the levels of inflammatory cytokines such asIL-6 and TNF-α in the liver and frontal cortex as well as serum LPS were significantly lower than in the BDL group. There is a correlation between the inflammatory processes and the neurological symptoms observed in HE post-BDL (5, 57). Aligned with previous studies, the data indicated elevated levels of ammonia in serum and CSF, along with heightened IL-6 and TNF-α, as well as reduced BDNF levels in the frontal cortex following BDL. Further, the PET scans indicate brain damage after BDL. The following factor s, in addition to the results of a behavioral test indicating motor dysfunction and memory deficits, suggest the presence of HE post-BDL. One study found that liver dysfunction results in increased ammonia, bile acids, and inflammation, which activate microglia and trigger neuroinflammation; probiotics can help mitigate these factors (58). Another study noted that consuming probiotics augmented the levels of BDNF (59). The current study indicates that combining the probiotic LGG with sorafenib in BDL rats lowered ROS and TNF-α levels in the frontal cortex, while frontal cortex BDNF levels did not differ significantly from the sham group—suggesting preservation of BDNF by this combination therapy. In contrast, all other groups revealed significant reductions in BDNF compared to sham group. These findings reflect a beneficial effect on BDNF expression consistent with prior reports, which correlates with enhanced motor function, diminished anxiety-like behavior, and improved cognition in behavioral tests relative to sorafenib alone. No significant difference was noted in BDNF levels between the PRO+SOR group and the SOR group. BDNF may still play a role in other brain regions or at different time points, and future studies should explore the full spectrum of molecular mediators underlying functional recovery.

In an open-field test, the sorafenib treatment group revealed higher distances traveled and center occupancy compared to the BDL group. The combined treatment of LGG and sorafenib led to significantly greater improvements in the measured parameters, including enhanced locomotor function and lowered anxiety levels, compared to sorafenib alone. In the shuttle box test, the Sor group did not exhibit a significant rise in step-through latency, indicating an absence of effect on fear memory. Nevertheless, the combination with LGG improved fear memory outcomes, aligning with findings from other studies. Thus, the integration of these two elements results in a synergistic outcome. Data from PET scans revealed that the BDL groups had lower 18FDG absorption compared to the sham group, reflecting brain damage and HE, in line with earlier findings (60). While LGG combined with low-dose sorafenib presented superior efficacy compared to either monotherapy, this study did not perform formal dose-response analyses to confirm synergy by established criteria. The enhanced additive effects observed here provide rationale for future dose-response studies to ascertain true synergistic interactions.

Conclusion

The current study indicated that combining sorafenib with the probiotic LGG may boost therapeutic effects against liver fibrosis and HE, primarily through regulation of the TLR4/NF-κB signaling pathway. This combination helps maintain gut barrier integrity, stabilizes the gut microbiota, and mitigates the harmful effects of lipopolysaccharides (LPS) and subsequent TLR4 activation. As a result, downstream NF-κB-mediated inflammatory responses are reduced, attenuating inflammation and tissue injury in both the liver and brain. Notably, the combination significantly lowered TNF-α levels in the frontal cortex compared to sorafenib alone, reflecting a reduction in neuroinflammation. These mechanistic insights provide a foundation for understanding how targeting inflammatory signaling and the gut-liver-brain axis can ameliorate disease outcomes. Further investigations should emphasize delineating these pathways in greater detail as well as validating the clinical potential of this combination treatment in patients with liver disease.

Acknowledgment

The results presented in this paper were part of a student thesis. The authors acknowledge the grant support of Tehran University of Medical Sciences. The authors would like to thanks and acknowledge Tehran University of Medical Sciences Preclinical Core Facility (TPCF), Tehran, Iran, for supporting and providing the *in vivo* Micro PET and SPECT imaging and image processing services for this research.

Data Availability

The data that support the findings of this study are available from the corresponding author upon reasonable request.

Ethics Approval

All procedures in this investigation were approved by the Tehran University of Medical Sciences Ethics Committee (IR.TUMS.AEC.1402.011) which corresponds to the national guidelines for animal care (NIH guidelines; Guide for the Care and Use of Laboratory Animals, NIH Publication 86-23).

Funding

This study was supported by Tehran University of Medical Sciences (grant no 1401-4-233-64077)

Authors' Contributions

T R, F N, and S A designed the experiments; T R, S A, SH H, M P, R G and, OR T performed experiments and collected data; T R, G A, and F N contributed to statistical analysis, manuscript preparation, interpretation of results, and discussed the results and strategy; F N supervised, directed, and managed the study; T R, G A, and F N drafted the Manuscript. T R, G A, S A, SH H, M P, R G ,OR T, and F N approved the final version to be published.

Conflicts of Interest

The authors have no relevant financial or non-financial interests to disclose.

Declaration

We have not used any AI tools or technologies to prepare this manuscript.

References

1. Roehlen N, Crouchet E, Baumert TF. Liver Fibrosis: Mechanistic Concepts and Therapeutic Perspectives. Cells. 2020;9:875.
2. Zhang S, Liu Q, He J, Li Y. Novel Therapeutic Targets in Liver Fibrosis. Front Mol Biosci. 2021;8:766855.
3. Parola M, Pinzani M. Liver fibrosis: Pathophysiology, pathogenetic targets and clinical issues. Mol Aspects Med. 2019;65:37-55.
4. Gallego-Durán R, Hadjihambi A, Ampuero J, Rose CF, Jalan R, Romero-Gómez M. Ammonia-induced stress response in liver disease progression and hepatic encephalopathy. Nat Rev Gastroenterol Hepatol 2024;21:774-791.
5. Claeys W, Van Hoecke L, Geerts A, Van Vlierberghe H, Lefere S, Van Imschoot G, *et al.* A mouse model of hepatic encephalopathy: bile duct ligation induces brain ammonia overload, glial cell activation and neuroinflammation. Sci Rep 2022;12:17558.
6. Miranda M, Morici JF, Zanoni MB, Bekinschtein P. Brain-derived neurotrophic factor: A key molecule for memory in the healthy and the pathological brain. Front Cell Neurosci 2019;13:363.
7. Chen X-F, Ji S. Sorafenib attenuates fibrotic hepatic injury through mediating lysine crotonylation. Drug Des Devel Ther 2023;16:2133-44.
8. Tang W, Chen Z, Zhang W, Cheng Y, Zhang B, Wu F, *et al.* The mechanisms of sorafenib resistance in hepatocellular carcinoma: Theoretical basis and therapeutic aspects. Signal Transduct Target Ther2020;5:87.
9. Wang Y, Gao J Fau - Zhang D, Zhang D Fau - Zhang J, Zhang J Fau - Ma J, Ma J Fau - Jiang H, Jiang H. New insights into the antifibrotic effects of sorafenib on hepatic stellate cells and liver fibrosis. J Hepatol 2010;53:132-144.
10. Tang W, Chen Z, Zhang W, Cheng Y, Zhang B, Wu F, *et al.* The mechanisms of sorafenib resistance in hepatocellular carcinoma: Theoretical basis and therapeutic aspects. Signal Transduct Target Ther 2020;5:87.
11. Nenu I, Baldea I, Coadă CA, Crăciun RC, Moldovan R, Tudor D, *et al. Lactobacillus rhamnosus* probiotic treatment modulates gut and liver inflammatory pathways in a hepatocellular carcinoma murine model. A preliminary study. Food Chem Toxicol 2024;183:114314.
12. Gou HZ, Zhang YL, Ren LF, Li ZJ, Zhang L. How do intestinal probiotics restore the intestinal barrier? Front Microbiol 2022 14;13:929346.

13. An L, Wirth U, Koch D, Schirren M, Drefs M, Koliogiannis D, *et al.* The role of gut-derived lipopolysaccharides and the intestinal barrier in fatty liver diseases. J Gastrointest Surg 2022 ; 26:671-683.
14. Liu YA-O, Chen K, Li F, Gu Z, Liu Q, He L, *et al.* Probiotic *Lactobacillus rhamnosus* GG prevents liver fibrosis through inhibiting hepatic bile acid synthesis and enhancing bile acid excretion in mice. Hepatology 2020;71:2050-2066.
15. Wang Y, Kirpich I, Liu Y, Ma Z, Barve S, McClain CJ, *et al.* *Lactobacillus rhamnosus* GG treatment potentiates intestinal hypoxia-inducible factor, promotes intestinal integrity and ameliorates alcohol-induced liver injury. Am J Pathol 2011;179:2866-2875.
16. Bai Y, Ma K, Li J, Li J, Bi C, Shan A. Deoxynivalenol exposure induces liver damage in mice: Inflammation and immune responses, oxidative stress, and protective effects of *Lactobacillus rhamnosus* GG. Food Chem Toxicol 2021;156:112514.
17. D'Mello C, Ronaghan N, Zaheer R, Dicay M, Le T, MacNaughton WK, *et al.* Probiotics improve inflammation-associated sickness behavior by altering communication between the peripheral immune system and the brain. J Neurosci 2015;35:10821-10830.
18. Hennenberg M, Trebicka J, Kohistani Z, Stark C, Nischalke H-D, Krämer B, *et al.* Hepatic and HSC-specific sorafenib effects in rats with established secondary biliary cirrhosis. Lab Invest 2011;91:241-251.
19. Wang Y, Gao J, Zhang D, Zhang J, Ma J, Jiang H. New insights into the antifibrotic effects of sorafenib on hepatic stellate cells and liver fibrosis. J Hepatol 2010;53:132-144.
20. Lucidi M, Marsan M, Pudda F, Pirolo M, Frangipani E, Visca P, *et al.* Geometrical-optics approach to measure the optical density of bacterial cultures using a LED-based photometer. Biomed Opt Express 2019;10:5600-5610.
21. Jafaripour L, Esmaeilpour K, Maneshian M, Bashiri H, Rajizadeh MA, Ahmadvand H, *et al.* The effect of gallic acid on memory and anxiety-like behaviors in rats with bile duct ligation-induced hepatic encephalopathy: Role of AMPK pathway. Avicenna J Phytomed 2022;12:425-438.
22. Takeuchi H, Iba M, Inoue H, Higuchi M, Takao K, Tsukita K, *et al.* P301S mutant human tau transgenic mice manifest early symptoms of human tauopathies with dementia and altered sensorimotor gating. PLoS One 2011;6:e21050.
23. Yang B, Sun T, Chen Y, Xiang H, Xiong J, Bao S. The role of gut microbiota in mice with bile duct ligation-evoked cholestatic liver disease-related cognitive dysfunction. Front Microbiol 2022;13:909461.
24. Cho I, Koo BN, Kam EH, Lee SK, Oh H, Kim SY. Bile duct ligation of C57BL/6 mice as a model of hepatic encephalopathy. Anesth Pain Med (Seoul) 2020;15:19-27.
25. Modaresi Movahed T, Jalaly Bidgoly H, Khoshgoftar Manesh MH, Mirzaei HR. Predicting cancer cells progression via entropy generation based on ARIMA and ARMA models. Int Commun Heat Mass Transf 2021;127:105565.
26. Yousefi-Manesh H, Rashidian A, Hemmati S, Shirooie S, Sadeghi MA, Zarei N, *et al.* Therapeutic effects of modafinil in ischemic stroke; possible role of NF-κB downregulation. Immunopharmacol Immunotoxicol 2019;41:558-564.
27. Shafie F, Nabavizadeh F, Shafie Ardestani M, Panahi M, Adeli S, Samandari H, *et al.* Sorafenib-loaded PAMAM dendrimer attenuates liver fibrosis and its complications in bile-duct-ligated rats. Can J Physiol Pharmacol 2019;97:691-698.
28. Domenicali M, Caraceni P, Giannone FA, Pertosa AM, Principe A, Zambruni A, *et al.* Cannabinoid type 1 receptor antagonism delays ascites formation in rats with cirrhosis. Gastroenterology 2009;137 1:341-349.
29. Jalilpiran Y, Tanideh N, Rahmdel S, Azarpira N, Mokhtari M, Mazloom Z. Protective effects of synbiotic soymilk fortified with whey protein concentrate and zinc sulfate against bile duct ligated-induced hepatic encephalopathy. Gastroenterol Hepatol Bed Bench 2020;13:64-76.
30. Sule RA-O, Rivera G, Gomes AA-O. Western blotting (immunoblotting): History, theory, uses, protocol and problems. Biotechniques 2023;75:99-114.
31. Wang X, Zhang L Fau - Goldberg SN, Goldberg Sn Fau - Bhasin M, Bhasin M Fau - Brown V, Brown V Fau - Alsop DC, Alsop Dc Fau - Signoretti S, *et al.* High dose intermittent sorafenib shows improved efficacy over conventional continuous dose in renal cell carcinoma. J Transl Med 2011;9:220
32. Hennenberg M, Trebicka J Fau - Kohistani Z, Kohistani Z Fau - Stark C, Stark C Fau - Nischalke H-D, Nischalke Hd Fau - Krämer B, Krämer B Fau - Körner C, *et al.* Hepatic and HSC-specific sorafenib effects in rats with established secondary biliary cirrhosis. Lab Invest 2011;91:241-251.
33. Bao Y-l, Wang L, Pan H-t, Zhang T-r, Chen Y-h, Xu S-j, *et al.* Animal and organoid models of liver fibrosis. Front Physiol 2021:12:666138.
34. Simicic D, Rackayova V, Braissant O, Toso C, Oldani G, Sessa D, *et al.* Neurometabolic changes in a rat pup model of type C hepatic encephalopathy depend on age at liver disease onset. Metab Brain Dis 2023;38:1999-2012.
35. Yuan S, Wei C, Liu G, Zhang L, Li J, Li L, *et al.* Sorafenib attenuates liver fibrosis by triggering hepatic stellate cell ferroptosis via HIF-1α/SLC7A11 pathway. Cell Prolif 2022;55:e13158.
36. Nenu I, Baldea I, Coadă CA, Crăciun RC, Moldovan R, Tudor D, *et al.* *Lactobacillus rhamnosus* probiotic treatment modulates gut and liver inflammatory pathways in a hepatocellular carcinoma murine model. A preliminary study. Food Chem Toxicol 2024 Jan:183:114314.
37. Hajiasgharzadeh K, Shanehbandi D, Karimi-Sales E, Alipour MR. Effects of nicotine on microRNA-124 expression in bile duct ligation-induced liver fibrosis in rats. BMC Pharmacol Toxicol 2024;25:27.
38. Yang YY, Lu R-S, Lee P-C, Yeh Y-C, Huang Y-T, Lee W-P, *et al.* Anti-VEGFR agents ameliorate hepatic venous dysregulation/microcirculatory dysfunction, splanchnic venous pooling and ascites of NASH-cirrhotic rat. Liver Int 2014;34:521-534.
39. Liu Y, Chen K, Li F, Gu Z, Liu Q, He L, *et al.* Probiotic *Lactobacillus rhamnosus* GG prevents liver fibrosis through inhibiting hepatic bile acid synthesis and enhancing bile acid excretion in mice. Hepatology 2020;71:2050-2066.
40. Uhlig M, Hein M, Habigt MA, Tolba RH, Braunschweig T, Helmedag MJ, *et al.* Cirrhotic cardiomyopathy following bile duct ligation in rats—a matter of time? Int J Mol Sci 2023;24:8147.
41. Aghaei I, Nazeri M, Shabani M, Mossavinasab M, Mirhosseini FK, Nayebpour M, *et al.* Erythropoietin ameliorates the motor and cognitive function impairments in a rat model of hepatic cirrhosis. Metab Brain Dis 2015;30:197-204.
42. Lupescu A, Shaik N, Jilani K, Zelenak C, Lang E, Pasham V, *et al.* Enhanced erythrocyte membrane exposure of phosphatidylserine following sorafenib treatment: An *in vivo* and *in vitro* study. Cell Physiol Biochem 2012;30:876-888.
43. Shafie F, Nabavizadeh F, Shafie Ardestani M, Panahi M, Adeli S, Samandari H, *et al.* Sorafenib-loaded PAMAM dendrimer attenuates liver fibrosis and its complications in bile-duct-ligated rats. Can J Physiol Pharmacol 2019;97:691-698.
44. Laschke MW, Dold S, Menger MD, Jeppsson B, Thorlacius H. Platelet-dependent accumulation of leukocytes in sinusoids mediates hepatocellular damage in bile duct ligation-induced cholestasis. Br J Pharmacol 2008;153:148-156.
45. Bocca C, Novo E, Miglietta A, Parola M. Angiogenesis and fibrogenesis in chronic liver diseases. Cell Mol Gastroenterol Hepatol 2015;1:477–488.
46. Zadorozhna M, Di Gioia S, Conese M, Mangieri D. Neovascularization is a key feature of liver fibrosis progression: anti-angiogenesis as an innovative way of liver fibrosis treatment. Mol Biol Rep 2020;47:2279-2288.
47. Ma R, Chen J, Liang Y, Lin S, Zhu L, Liang X, *et al.* Sorafenib: A potential therapeutic drug for hepatic fibrosis and its outcomes. Biomed Pharmacother 2017:88:459-468.
48. Wang L, Liu W-Q, Broussy S, Han B, Fang H. Recent advances of anti-angiogenic inhibitors targeting VEGF/VEGFR axis. Front Pharmacol 2024 Jan 4:14:1307860.

49. Elçi MP, Fatsa T, Sinem K, Ersoy N, Alpay M, Özgürtaş T. Overview of the angiogenic effect of probiotics (*Lactobacillus acidophilus* and *Lactobacillus rhamnosus*) at human umbilical vein endothelial cells. J Health Sci Med 2022;5:765-770.
50. Engelmann C, Sheikh M, Sharma S, Kondo T, Loeffler-Wirth H, Zheng YB, *et al*. Toll-like receptor 4 is a therapeutic target for prevention and treatment of liver failure. J Hepatol 2020;73:102-112.
51. Fang Y, Zhou L, Hu X, Guo J, Liao J, Zhang Z. TLR4-MyD88-NF-κB signaling pathway contributes to the progression of secondary hepatic injury and fibrosis in hepatolithiasis. Eur J Inflamm 2021;19:1-12.
52. Li X, Xu M, Shen J, Li Y, Lin S, Zhu M, *et al*. Sorafenib inhibits LPS-induced inflammation by regulating Lyn-MAPK-NF-kB/AP-1 pathway and TLR4 expression. Cell Death Discov 2022;8:281.
53. Wang Y, Liu Y, Kirpich I, Ma Z, Wang C, Zhang M, *et al*. *Lactobacillus rhamnosus* GG reduces hepatic TNFα production and inflammation in chronic alcohol-induced liver injury. J Nutr Biochem 2013;24:1609-1615.
54. Hong M, Kim SW, Han SH, Kim DJ, Suk KT, Kim YS, *et al*. Probiotics (*Lactobacillus rhamnosus* R0011 and acidophilus R0052) reduce the expression of toll-like receptor 4 in mice with alcoholic liver disease. PLoS One 2015;10:e0117451.
55. Li H, Shi J, Zhao L, Guan J, Liu F, Huo G, *et al*. Lactobacillus plantarum KLDS1.0344 and *Lactobacillus acidophilus* KLDS1.0901 mixture prevents chronic acoholic liver injury in mice by Protecting the Intestinal Barrier and Regulating Gut Microbiota and Liver-Related Pathways. J Agric Food Chem 2021;69:183-197.
56. Zhou M, Lv J, Chen X, Shi Y, Chao G, Zhang S. From gut to liver: Exploring the crosstalk between gut-liver axis and oxidative stress in metabolic dysfunction-associated steatotic liver disease. Ann Hepatol 2025;30:101777.
57. Thanapirom K, Treeprasertsuk S, Choudhury A, Verma N, Dhiman RK, Al Mahtab M, *et al*. Ammonia is associated with liver-related complications and predicts mortality in acute-on-chronic liver failure patients. Sci Rep 2024; 14:5796.
58. Giuli L, Maestri M, Santopaolo F, Pompili M, Ponziani FR. Gut microbiota and neuroinflammation in acute liver failure and chronic liver disease. Metabolites 2023;13:772.
59. Shamsipour S, Sharifi G, Taghian F. Impact of interval training with probiotic (L. plantarum / Bifidobacterium bifidum) on passive avoidance test, ChAT and BDNF in the hippocampus of rats with Alzheimer's disease. Neurosci Lett 2021:756:135949.
60. Mosso J, Yin T, Poitry-Yamate C, Simicic D, Lepore M, McLin VA, *et al*. PET CMR(glc) mapping and (1)H-MRS show altered glucose uptake and neurometabolic profiles in BDL rats. Anal Biochem 2022; 647:114606.